

Arctic warming: Evolution and spreading of the 1990s warm event in the Nordic seas and the Arctic Ocean

Michael J. Karcher, Rüdiger Gerdes, Frank Kauker, and Cornelia Köberle

Alfred Wegener Institute for Polar and Marine Research, Bremerhaven, Germany

Received 11 December 2001; revised 22 July 2002; accepted 14 October 2002; published 18 February 2003.

[1] Observations in the Arctic Ocean revealed changes in oceanic temperature, salinity and ice cover of the 1990s as compared with earlier data. With a numerical model, we favorably reproduce the development and subsequent propagation of temperature anomalies in water of Atlantic origin in the 1980s and 1990s. These propagated into the Arctic Ocean via the Barents Sea and the Fram Strait. Two warm anomalies entered the Arctic Ocean through these passages. While the first smaller anomaly only warmed up the western Eurasian Basin, the second large anomaly spread far into the eastern Eurasian Basin and across the Lomonosov Ridge into the western Arctic basins. Intensified boundary currents during the high NAO state in the first half of the 1990s significantly influenced the amplitude and speed of propagation of the temperature anomalies inside the Arctic Ocean. In contrast to the notion of a continuous warming process during the 1990s, our model results suggest the warming of the Atlantic Layer in the Arctic Ocean occurred in the form of events. The event with the largest anomalous heat input during the modeled period entered the Arctic between 1989 and 1994. It is possible to trace back the additional heat input into the Arctic to an increased volume inflow via the Faroer-Scotland passage and reduced heat loss to the atmosphere in the early 1990s. After a weaker warm inflow in the second half of the 1990s, the most recent observations and the model results point to a recurring warm anomaly in the inflow from 1999 onward.

INDEX TERMS: 4207 Oceanography: General: Arctic and Antarctic oceanography; 4215 Oceanography: General: Climate and interannual variability (3309); 4255 Oceanography: General: Numerical modeling; 4536 Oceanography: Physical: Hydrography; *KEYWORDS:* arctic warming, Atlantic Layer, Arctic Ocean variability, coupled ice-ocean model, Nordic Sea exchanges

Citation: Karcher, M. J., R. Gerdes, F. Kauker, and C. Köberle, Arctic warming: Evolution and spreading of the 1990s warm event in the Nordic seas and the Arctic Ocean, *J. Geophys. Res.*, 108(C2), 3034, doi:10.1029/2001JC001265, 2003.

1. Introduction

[2] Hydrographic measurements in the Arctic Ocean from the recent decade have revealed large changes in the thermohaline structure which commenced in the early 1990s: The core of the Atlantic Water layer in the Eurasian Basin has been found to be warmer by more than 1° in the boundary current along the Siberian slope when compared to historical data [Quadfasel *et al.*, 1991; Grotefendt *et al.*, 1998]. An intense observational effort in the Canadian and Makarov basins (see Figure 1) uncovered that the front which divides Atlantic and Pacific origin watermasses had shifted from the Lomonosov Ridge to the Alpha and Mendeleev Ridge [Carmack *et al.*, 1995; McLaughlin *et al.*, 1996; Morison *et al.*, 1998; Swift *et al.*, 1996]. The reasons for the observed warming of the Atlantic layer and the frontal shift are under debate.

[3] The increase of the advection of atmospheric heat into the Nordic Seas in the early 1990s occurred in parallel with a rising North Atlantic Oscillation (NAO) index, and hence a reduced oceanic heat loss to the atmosphere [see, e.g., Dick-

son *et al.*, 2000]. This in turn would allow warmer Atlantic Water to intrude into the Arctic Ocean. A model study by Zhang *et al.* [1998] on the other hand concludes that the warming and salinification of the Arctic Ocean is the result of an increased volume inflow of Atlantic Water, mainly via the Barents Sea route. Häkkinen and Geiger [2000] investigate the dominant modes of variability of the barotropic streamfunction in a model simulation using Empirical Orthogonal Function (EOF) analysis. They find an intensification of Atlantic volume inflow into the Arctic in the early 1990s associated with the first mode which explains about two thirds of the variance. The intensity of this inflow is unprecedented in the 5 decades under investigation. In a study combining numerous atmospheric and oceanic observations and modeling results, Dickson *et al.* [2000] conclude that the Arctic warming of the early 1990s seems to be a combination of warmer and probably stronger inflow of both Atlantic Water branches into the Arctic Ocean.

[4] Further change is reported from the water above the Atlantic Layer in the Arctic. A salinification of the halocline in the eastern Eurasian Basin took place in the early nineties, reducing the density gradient between the mixed layer and the Atlantic Water layer [Steele and Boyd, 1998]. This might be due to a shift of pathways of Siberian river runoff

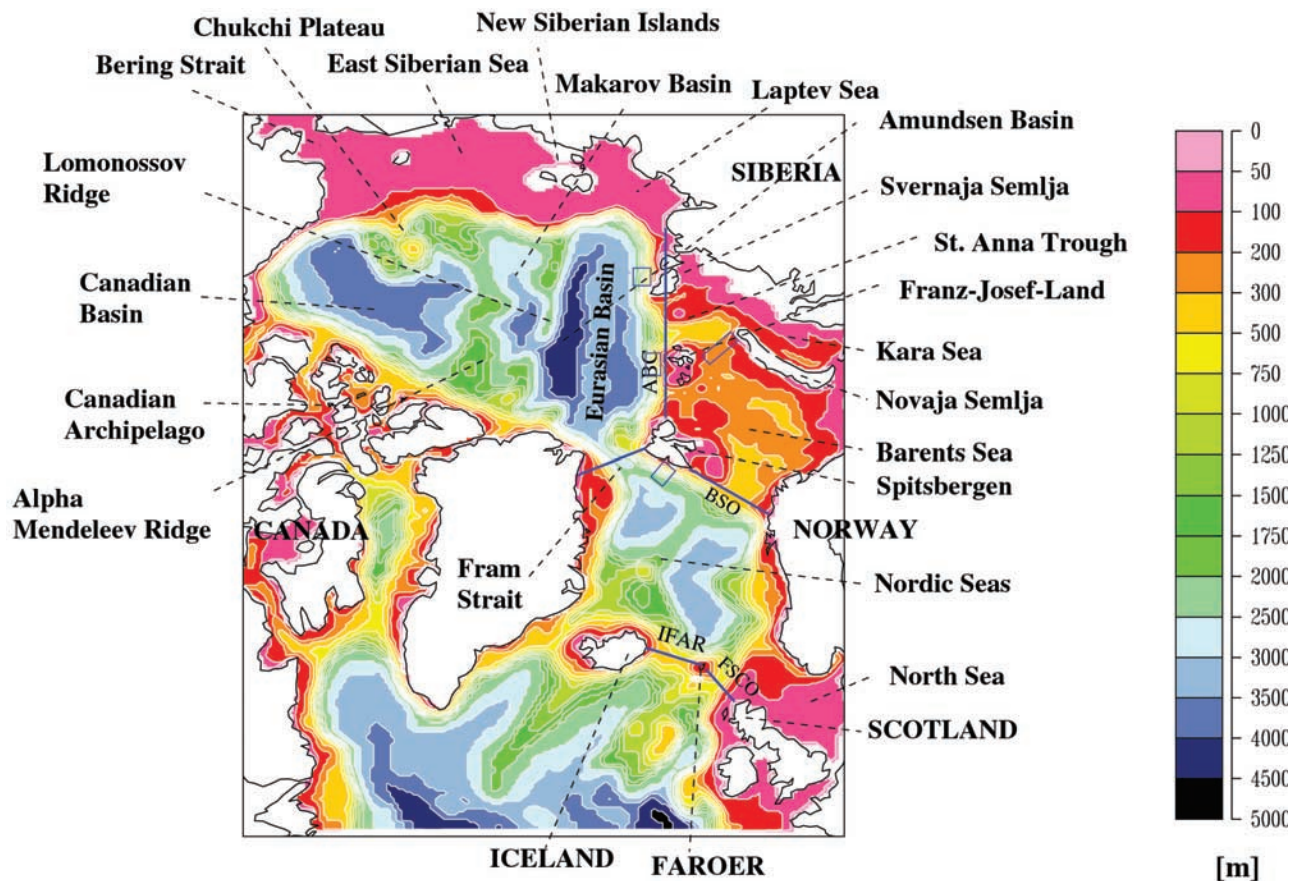


Figure 1. Bottom topography used for the current model simulation. The colored straight lines depict sections used for diagnostic purposes in the text. Small blue boxes show areas for constructing averaged time series of Atlantic Water core temperatures.

from a poleward direction to a cyclonic path along the Siberian Shelves during the 1990s [Steele and Boyd, 1998; Dickson, 1999; Maslowski *et al.*, 2001]. Johnson and Polyakov [2001] report model results in which the changes in wind stress patterns over the eastern Eurasian shelves indeed do lead to less advection of river runoff into the eastern Eurasian Basin, a reduced ice cover over the Laptev Sea and an increased brine rejection. Part of the observed changes seem to be driven by the decreasing atmospheric pressure of the Beaufort High, which started at the end of the 1980s [Walsh *et al.*, 1996]. This led to a reduction of the anticyclonic windstress pattern over the Arctic.

[5] Surface air temperatures in the Arctic and the Nordic Seas have increased in parallel with the phase of strong NAO in the late 1980s/early 1990s [Furevik, 2001; Rigor *et al.*, 2000]. Several authors discussed whether an increased heat flux from the warmer Atlantic Water layer to the surface may be a reason for the observed thinning of the ice cover found to occur in the Eurasian Basin and above the Lomonosov Ridge in the 1990s [Furevik, 2001; Rigor *et al.*, 2000]. C. Köberle and R. Gerdes (Causes of arctic sea ice volume variability, submitted to *Journal of Climatology*, 2002) (hereinafter referred to as Köberle and Gerdes, submitted manuscript, 2002) on the other hand argue that from model results they find no indication for an important role of ocean-ice heat fluxes for the changes in sea ice thickness of the central Arctic. Instead they claim shifts in ice drift pattern and atmospheric temperatures as respon-

sible for the observed ice thickness changes, in accordance with results from Holloway and Sou [2001].

[6] In the following we use a numerical coupled ice-ocean model as a tool to better understand some of the above changes observed in the Arctic Ocean. For the present investigation we focus on the history of the intrusion of Atlantic origin water into the Arctic Ocean between 1979 and 1999. After a description of the model and the experimental design in section 2, we will present the model results in sections 3 and 4. The modeled development of the Atlantic Water core temperatures in the Arctic Ocean are compared with observations. Subsequently, the temporal history of heat and volume fluxes are analyzed for the Arctic Ocean and the Nordic Seas, and heat balances are discussed. Finally we end with our conclusions on the sources for the observed and modeled warming in section 5.

2. Model Description and Experimental Design

[7] The ocean model used for the present investigation derives from the Geophysical Fluid Dynamics Laboratory modular ocean model MOM-2 [Pacanowski, 1995]. For the advection of tracers a FCT-scheme [Zalesak, 1979; Gerdes *et al.*, 1991] is employed, which is characterized by a low implicit diffusion and avoids false extrema (“overshooting”) in advected quantities. Friction is implemented as a biharmonic diffusion of momentum with a horizontal diffusion coefficient of $-0.5 \times 10^{21} \text{ cm}^4 \text{ s}^{-1}$. Vertical viscosity is taken

to be constant with a friction coefficient of $10 \text{ cm}^2 \text{ s}^{-1}$. The bottom drag coefficient is 1.2×10^{-3} . The model domain encloses the northern North Atlantic, the Nordic Seas and the Arctic Ocean (Figure 1). The southern model boundary approximately runs along 50°N . Here, an open boundary condition has been implemented following *Stevens* [1991]. This boundary condition allows the outflow of tracers and the radiation of waves. At inflow points determined by the model, temperature and salinity are specified according to climatology [*Levitus et al.*, 1994a, 1994b]. The baroclinic part of the horizontal velocity is calculated from a simplified momentum balance while the barotropic velocities normal to the boundary are specified from a lower resolution version of the model that covers the entire North Atlantic (*Köberle and Gerdes*, 2002). Other boundaries are treated as closed walls. The horizontal resolution is $0.25^\circ \times 0.25^\circ$ on a rotated spherical grid which is introduced to avoid numerical difficulties at the pole. The rotation of the grid shifts the equator to the geographical 30°W meridian and the pole to 60°E on the geographical equator. In the vertical, the model has 30 unevenly spaced levels. Bottom topography is based on the Etopo5 data set of the National Geophysical Data Center. Modifications were made to open two channels in the Canadian Archipelago that connect the Arctic Ocean with Baffin Bay.

[8] The ocean model is coupled to a dynamic-thermodynamic sea ice model [*Hibler*, 1979; *Harder et al.*, 1998] which employs a viscous-plastic rheology. The thermodynamics follow *Semtner* [1976]. Freezing and melting are calculated by solving the energy budget equation for a single ice layer with optional snow cover. The freezing point of sea water is salinity dependent. The sea ice and ocean models use the same time step and the same horizontal grid and the calculation of nonlinear ice-ocean momentum fluxes are based on ocean currents which are temporally smoothed using moving four-daily means. Outflow of ice out of the domain is allowed at the southern boundary and at Bering Strait. The models are coupled following the procedure devised by *Hibler and Bryan* [1987]. The surface heat flux is calculated from standard bulk formulae using prescribed atmospheric data and sea surface temperature predicted by the ocean model.

[9] Initial conditions for potential temperature and salinity were taken from the Arctic Ocean EWG-climatology for winter [*NSIDC Environmental Working Group*, 1997]. Where the model domain exceeds the EWG-climatology domain, the climatology of *Levitus et al.* [1994a, 1994b] has been used. The model is forced with daily mean 2-m air temperature and dew point temperature, cloudiness, precipitation, wind speed and surface windstress. For the first 20 years of spin-up, a climatology of these atmospheric data is used, which consists of a climatological mean seasonal cycle of the period 1979–1993 with added typical daily variability (OMIP-climatology) [*Röske*, 2001]. After the spin-up, the forcing consists of daily mean atmospheric data from the ECMWF reanalysis for the period 1979–1993 [*Gibson et al.*, 1997]. For the period 1994–1999, 2-m air temperature and dew point temperature, wind speed and surface wind stress are taken from the ECMWF analysis. Cloudiness and precipitation data for this period are taken from the OMIP-climatology. Freshwater influx from rivers is not explicitly included. To account for river run-off and diffuse run-off from the land, as well as to include the effect of flow into the Arctic through Bering Strait

on the salinity, a restoring flux (with an adjustment timescale of 180 days) is added to the surface freshwater flux. The restoring flux is calculated in reference to observed data from the EWG-atlas [*NSIDC Environmental Working Group*, 1997] for the Arctic Ocean and the Nordic Seas and *Levitus et al.* [1994a, 1994b] for the rest of the domain. The effect of the restoring flux on the surface salinity for this and other Arctic Ocean models is documented by *Steele et al.* [2001]. The entire hindcast integration covers a period of 21 years (1979–1999) after spin-up.

3. Atlantic Water Temperatures in the Arctic Ocean 1979–1999

[10] Since hydrographic measurements in the central Arctic are still sparse and necessarily cover space and time inhomogeneously, the comparison of the model results with observations is difficult. A check of the consistency of the model results with available observations is done here by overlaying subsampled Atlantic Water core temperatures from published observations onto the respective modeled temperature patterns for the appropriate time (Figure 2). In the following section, we will first discuss the development of the core temperatures in the Atlantic Water layer according to those observations. In a second step, the modeled core temperatures for the period in question will be presented and compared with the observations.

3.1. Observations

[11] The history of temperatures of Atlantic Water prior to entering the Arctic Ocean through Fram Strait is depicted by a time series of 50–500 m depth averaged temperatures near Sørkapp (the south cape of Spitsbergen) [*Dickson et al.*, 2000]. It reveals two periods of anomalously high temperatures of the northward flowing Atlantic Water. The first warm period (WSC-W1) took place in the early to middle 1980s, followed by a cold period between 1985 and 1987 (WSC-C1). From 1988 to 1995 a second warm period (WSC-W2) was characterized by even higher temperatures than the first warm period (Figure 3a). The naming of the cold and warm phases is done in a fashion similar to that of *Furevik* [2001].

[12] First published observations of downstream Atlantic Water layer temperatures in the period of 1979–1980 stem from the YMER 80 expedition in 1980. Their data cover the core of the Atlantic Water layer at the Barents Sea slope between Spitsbergen and Franz-Josef-Land right after passing Fram Strait [*Rudels*, 1986] with a potential temperature of $1.5\text{--}2^\circ\text{C}$ (Figure 2a). *Perkin and Lewis* [1984] report temperatures of around 2.2°C in the Atlantic Water core northeast of Spitsbergen in 1981 (not shown). Three years later during the cruise ARKII/3 with POLARSTERN, *Koltermann and Lüthje* [1989] found Atlantic Water core temperatures in excess of 3°C (Figure 2b), seemingly reflecting the phase of warm Atlantic Water found in the West Spitsbergen Current in the early to middle 1980s (WSC-W1) (Figure 3a). Also, the following cold phase of the West Spitsbergen Current (WSC-C1) (Figure 3a) is apparent in downstream observations: In 1987, core temperatures of below 2°C northeast of Spitsbergen were found by *Anderson and Jones* [1992] (Figure 2c). One year later, around 2.5°C were reported by *Steele et al.* [1995] during the CEAREX88 drift in 1988 and by *Muench et al.* [1992]

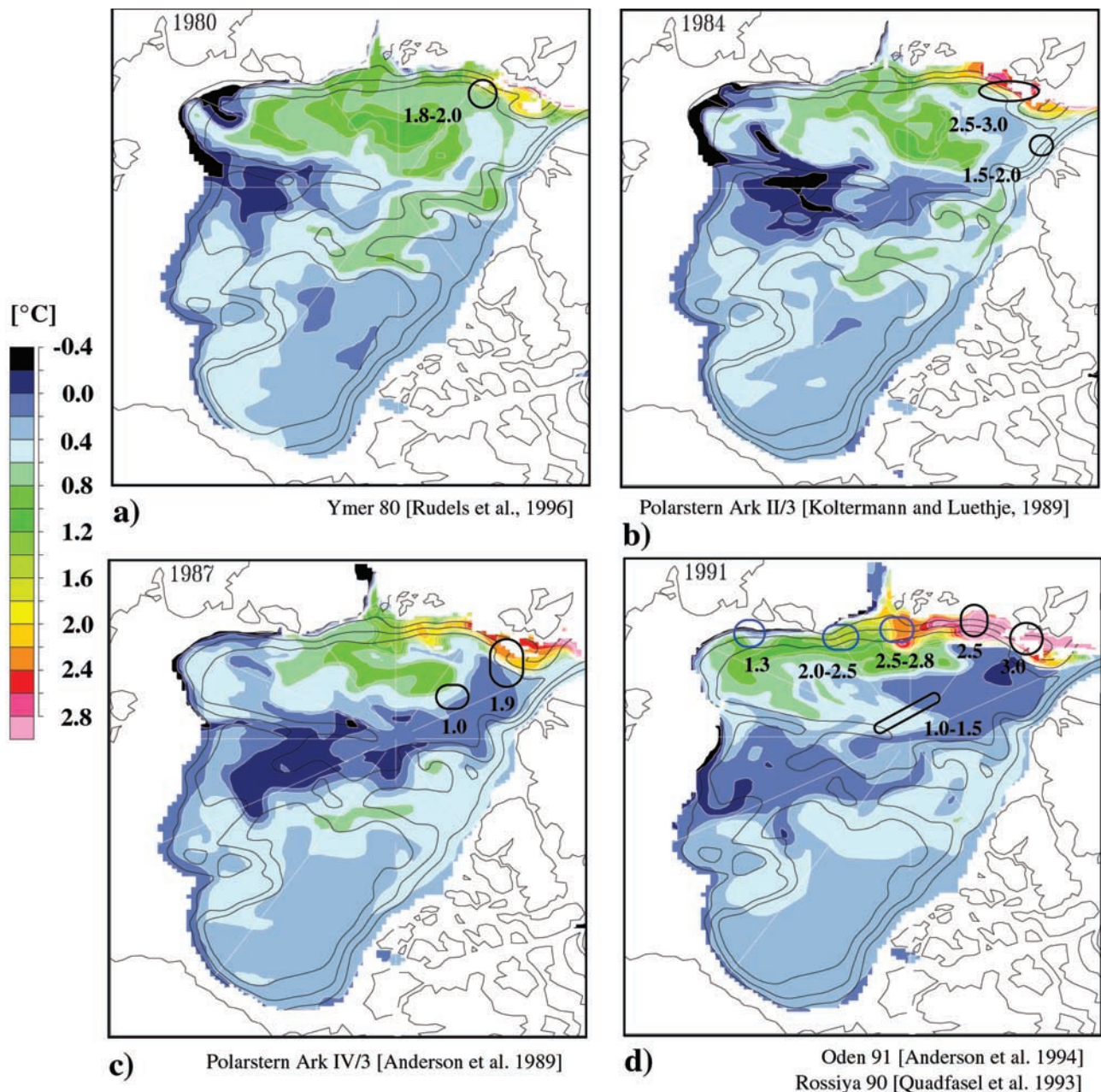


Figure 2. Subsampled September means of the modeled Atlantic Water core temperature between 1980 and 1999 defined as the maximum temperature in the water column. Areas shallower than 500 m and profiles with a maximum temperature shallower than 150 m have been omitted. Numbers show observed core temperatures at the indicated locations from published observations from the same year (see citations below each panel). Numbers and text in blue refer to observations made 1 year earlier. For the observations, only single locations from the published data are shown. The reference “website” refers to <http://www.ldeo.columbia.edu/SCICEX/Media/3tdif.jpg>.

from winter expeditions to the area north of Spitsbergen in March/April 1989 (not shown).

[13] It was in 1990 that *Quadfasel et al.* [1991] found first observational evidence of unusually warm water in the Atlantic Water boundary current further east at the northern slope of the Kara Sea (Figure 2d) when comparing their observations with climatological data [*Gorshkov*, 1980] and modern synoptic data [*Perkin and Lewis*, 1984; *Anderson et al.*, 1989]. At the same time, a temperature increase in the upstream West Spitsbergen Current marks a second warm

anomaly of Atlantic Water south of Fram Strait (WSC-W2) (Figure 3a). Unfortunately, only very few measurements cover the Atlantic Water core north of the Barents Sea during the early 1990s. *Anderson et al.* [1994] report a maximum core temperature of above 3°C at the northeastern tip of Spitsbergen in 1991 gained from the ODEN 91 expedition (Figure 2d). In 1993, *Schauer et al.* [1997] found rather warm core temperatures of 2.5°–3°C north of the western Barents Sea (Figure 2e). The temperatures in the boundary current farther east, north of the Laptev Sea, were

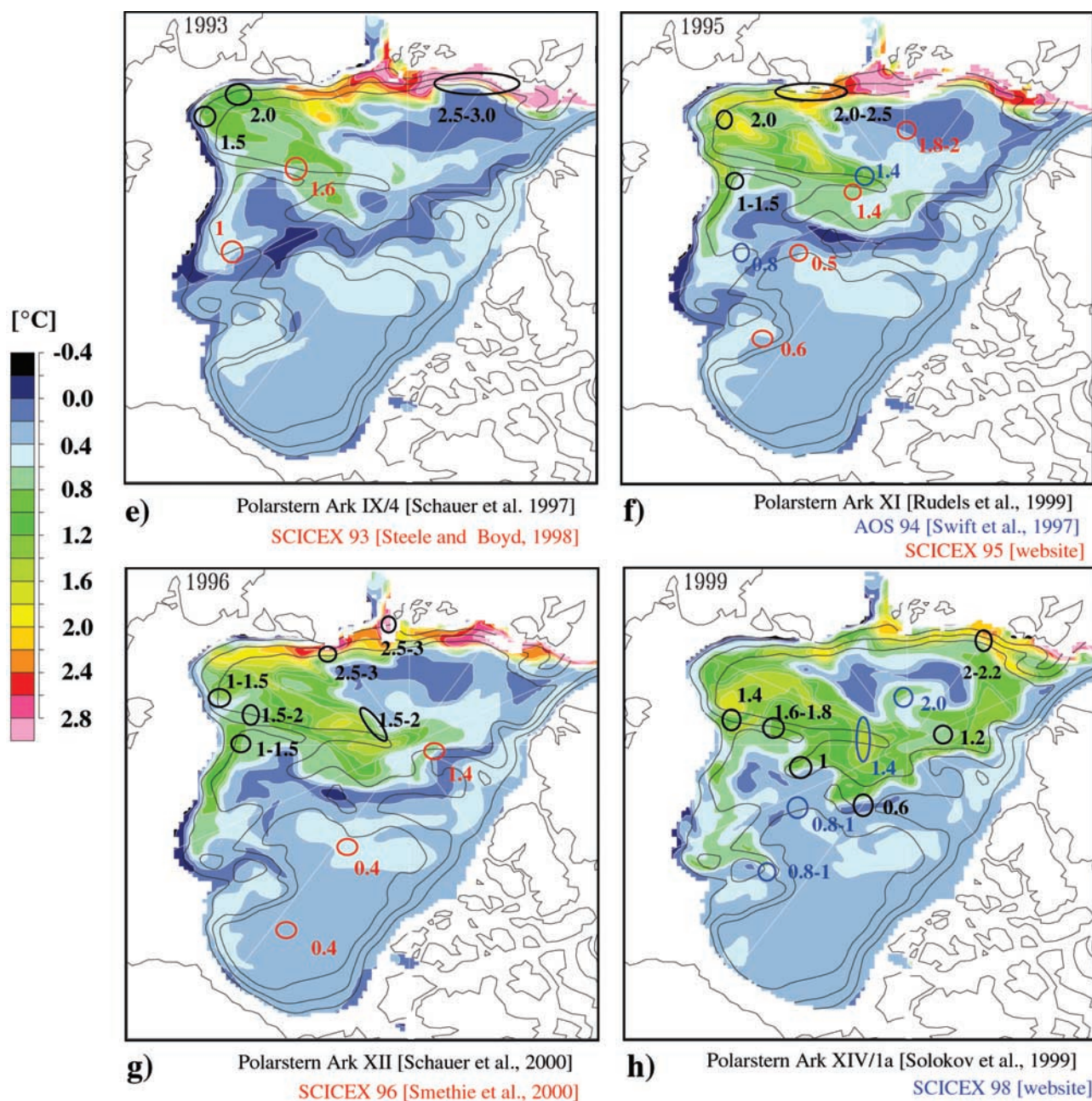


Figure 2. (continued)

between 1.5°C and 2°C [Schauer et al., 1997]. In the same year, anomalously warm water also had been found beyond the Lomonossov Ridge, as reported from the CCGS Henry Larsen cruise [McLaughlin et al., 1996] and from submarine based observations during SCICEX93 [Steele and Boyd, 1998; Morison et al., 1998]. These authors report core temperatures of about 1.6°C above the Lomonossov Ridge between the New Siberian Islands and the North Pole and up to 1°C on the continental slope of the Makarov Basin (Figure 2e) indicating a progressive nature of the warming in comparison to historical data. Its movement with the boundary currents is supported by further warming of the branches along the Kara and Laptev Sea slopes and the continental slope in the Makarov Basin in 1995 [Rudels et al., 2000] (Figure 2f) and 1996 [Schauer et al., 2002]

(Figure 2g) and at the North Pole in 1994 [Swift et al., 1996] and 1996 [Schauer et al., 2002] (Figures 2g and 2f).

[14] Evidence for a continuation of the advection of the anomalously warm water along the paths from the North Pole to northern Fram Strait and along the continental slope in the Canadian Basin after 1995 comes from the SCICEX98 cruises (SCICEX website, 2000, <http://www.ldeo.columbia.edu/SCICEX/Media/3tdif.jpg>) (Figure 2g). Core temperatures at the slope of Chukchi Plateau were in excess of 0.8°C in 1998. A change in the upstream situation seems to have occurred, however, in the second half of the 1990s. Measurements from the SCICEX98 cruise (SCICEX website, 2000) and the Polarstern cruise ARK XIV [Solokov et al., 1999] give no indication for a further core temperature rise along the Lomonossov Ridge between Siberia and the North Pole (Figure 2h).

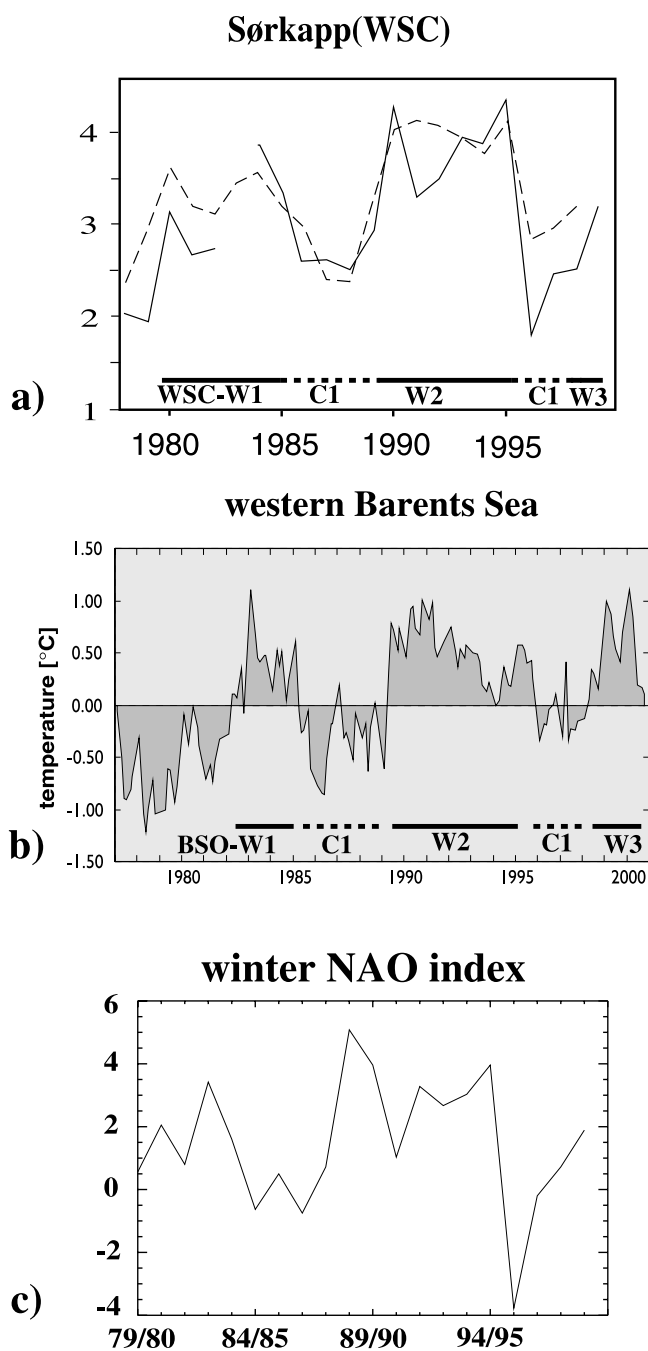


Figure 3. Observed time series of Atlantic Water temperature (a) in August–September integrated from 50–500 m depth in the West Spitsbergen Current (WSC) at the southern tip of Spitsbergen (Sørkapp) at two locations (9°E, solid line; and 11°E, dashed line)(adapted from Dickson *et al.* [2000]) and (b) from the western Barents Sea (courtesy of H. Loeng, IMR Bergen, 2001). For both panels, periods of warm and cold anomalies have been marked. (c) Normalized winter NAO index after Hurrell [1995]).

[15] We do not know how the Atlantic Water core temperature has developed further upstream, since no data are available from the Siberian slope between Franz-Josef-Land and the Lomonossov Ridge for the second half of the 1990s. The core temperature northeast of Fram Strait in 1999, however, was observed with 2–2.2°C [Sokolov *et al.*,

1999] (Figure 2h), which is as low as during the cold period years 1987/1988. Also, the West Spitsbergen Current time series even further upstream is suggestive of a cooler period after 1995 for the inflow of Atlantic Water (WSC-C2). More recently, after 1998, observations from Fram Strait indicate a return to warmer conditions in the Atlantic Water inflow (WSC-W3) (U. Schauer, personal communication, 2001).

[16] When timing and amplitude of observed temperatures in the Atlantic Layer of the Arctic Ocean are combined with time series of temperature in the West Spitsbergen Current, a strong upstream influence on the Arctic boundary current temperatures seems evident [see also, e.g., Swift *et al.*, 1996]. The high correlation of the WSC and western Barents Sea temperatures with the winter NAO index can easily be seen by comparing Figures 3a and 3b with Figure 3c [see also Dickson *et al.*, 2000]. Due to the sparseness of observation, however, a consistent picture of the temperature evolution of the entire Atlantic Layer over the last decades is not possible. Also, the relative contribution of the Fram Strait and Barents Sea branches are not known, and thus no conclusion on the causes for the observed development can be drawn at this stage.

3.2. Model Results and Data Comparison

[17] In this section we will present the evolution of the Atlantic Layer core temperatures as modeled in the hindcast experiment. We will compare the results with the observations referenced in the previous section. As in the previous section we refer to time series of Atlantic Water temperatures from upstream locations (Figure 4). However, since the model provides data about both sources of water for the Atlantic Layer: the Fram Strait Branch Water (FSBW) and the Barents Sea Branch Water (BSBW); we will discuss both.

[18] In 1980 the modeled maximum temperatures of the Atlantic Water core just northeast of the Fram Strait gap were about 2°C, in accordance with the observations. The remainder of the Eurasian Basin was characterized by Atlantic Water core temperatures below 1.5°C, a temperature level which is determined by the situation at the end of the 20 years spin-up phase (Figure 2a). In the mid-1980s a warming of the boundary current in the western Eurasian Basin set in, starting from the inflow at Fram Strait (Figure 2b). Maximum core temperatures reached about 3°C north of Spitsbergen comparable to observations. The source of the warm water was the propagation of a warm anomaly (WSC-W1) from the upstream West Spitsbergen Current which is apparent in a temperature time series from 50 to 500 m depth near Sørkapp (southwest of Spitsbergen) (Figure 4a). This time series derived from the model compares well with observed data from this area (Figure 3a). The eastward propagation velocity of the warm anomaly along the Barents Sea slope was slow and unsteady. The anomaly reached Franz-Josef-Land in the second half of the 1980s without passing beyond (Figure 2c).

[19] Between 1985 and 1988 the modeled temperatures north of Spitsbergen reduced again to values similar to the early 1980s (Figure 2c). This feature, which is well captured by the model when compared with observations, is a consequence of the inflow of colder water with the West Spitsbergen Current (WSC-C1) (Figure 4a).

[20] In 1990 a swift warm plume of Atlantic Water with anomalously warm core temperatures started penetrating the eastern Eurasian Basin along the shelf slope and reached the

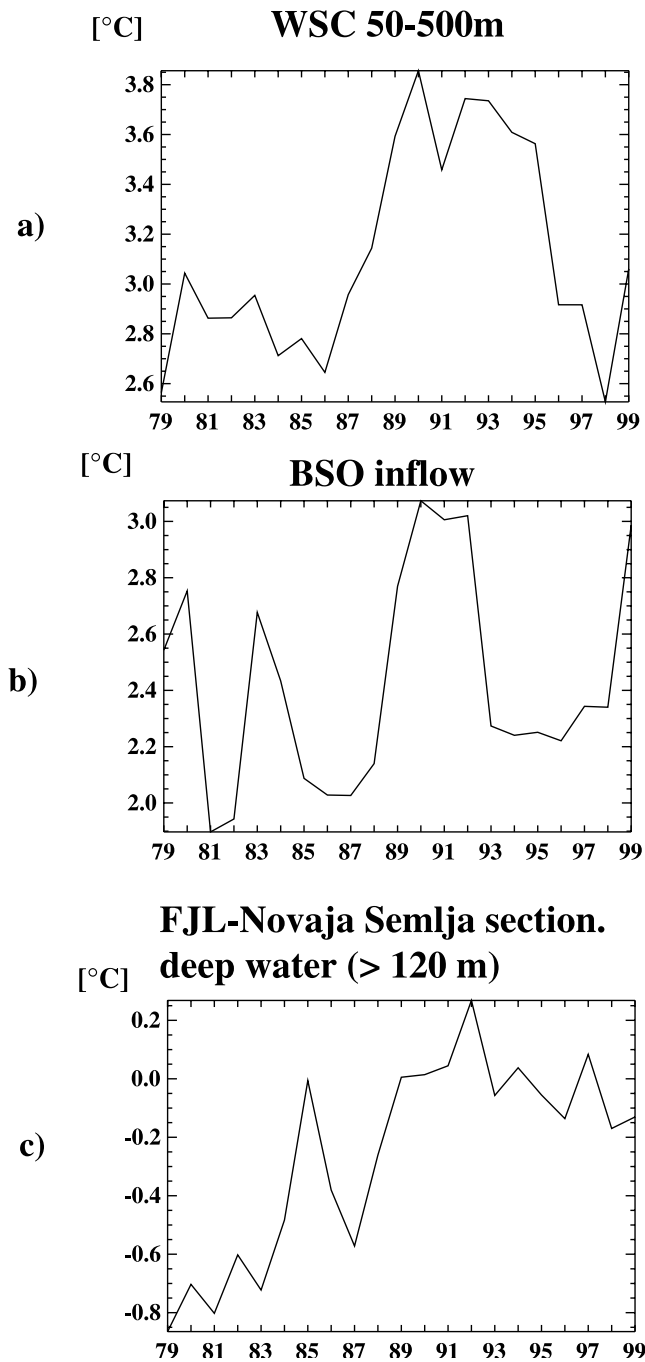


Figure 4. Time series of simulated yearly mean Atlantic Water temperatures along the path of Atlantic Water (a) in the West Spitsbergen Current (WSC) at 80°N (depth: 50–500 m), (b) vertically integrated along the southern part of the Barents Sea Opening (BSO) section, and (c) vertical mean of deep water (>120 m) moving northeastward at the southern end of the section Franz-Josef-Land to Novaja Semlja.

longitude of Svernaja Semlja. Our model results indicate that this first phase of warming in the eastern Eurasian Basin was created by an intense stirring of the cyclonic boundary current in the entire Arctic basins which set in around 1988/1989, as is depicted in time series of velocities in the boundary current from 350 m depth at the slope north of Franz-Josef-Land (Figure 5a) and northeast of Svernaja

Semlja (Figure 5b). Also, around 1989/1990 an increase in the Atlantic Water temperature of the West Spitsbergen Current took place (WSC-W2), visible in observations and model results (Figures 3a and 4a) which lead to a rise in the Atlantic Water core temperature of the eastward flowing boundary current east of Spitsbergen (Figure 2d). The temperature of the inflowing water remained high from 1990 to 1995 (Figure 4a). Due to the length of this warm period and the increased velocity of the cyclonic boundary current after 1990 a warm anomaly of large lateral extent swiftly proceeded eastward (Figures 2d–2g).

[21] To further elucidate the nature of this early warming phase, we calculated the contributions of means and anomalies of temperature (\bar{T} , T') and velocity (\bar{v} , v') to the local horizontal advection of heat integrated over 100–300 m depth of the water column,

$$c_p \rho v T = c_p \rho \{ \bar{v} \bar{T} + v' T' + \bar{v} T' + v' \bar{T} \}.$$

[22] In 1990 an anomalously high speed of the alongslope boundary current was evident from Fram Strait to Svernaja Semlja, contributing to a large horizontal heat transport (Figure 6a). A contribution of anomalous temperature did not occur in the boundary current east of Franz-Josef-Land, but existed for the Atlantic derived water which crossed the

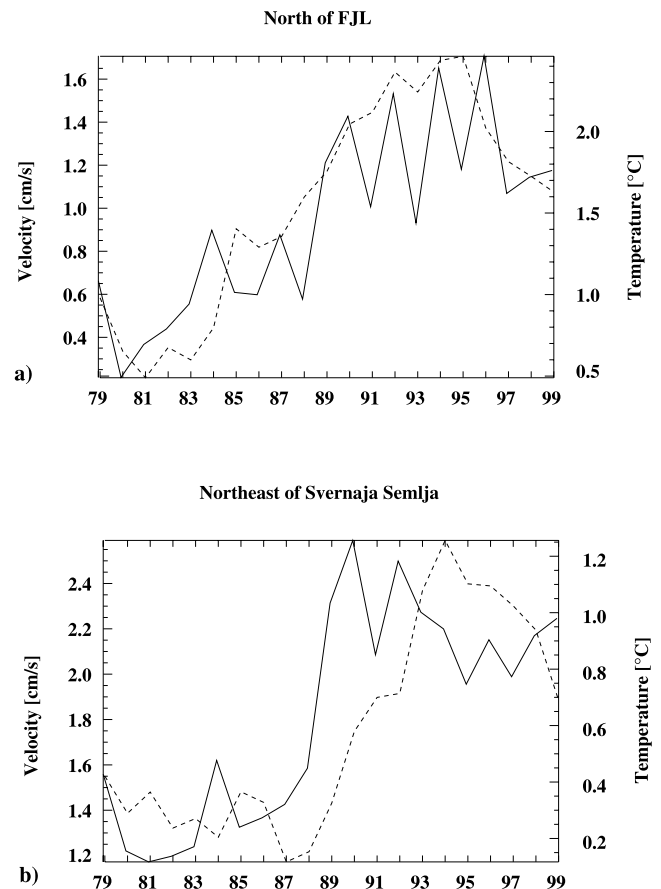


Figure 5. Monthly mean eastward velocities (solid lines) and temperatures (dashed lines) at 350 m depth in the boundary current at the Siberian Shelf slope (a) north of Franz-Josef-Land and (b) northeast of Svernaja Semlja. The velocities are an areal mean representing the cores of the boundary current (see small boxes in Figure 1).

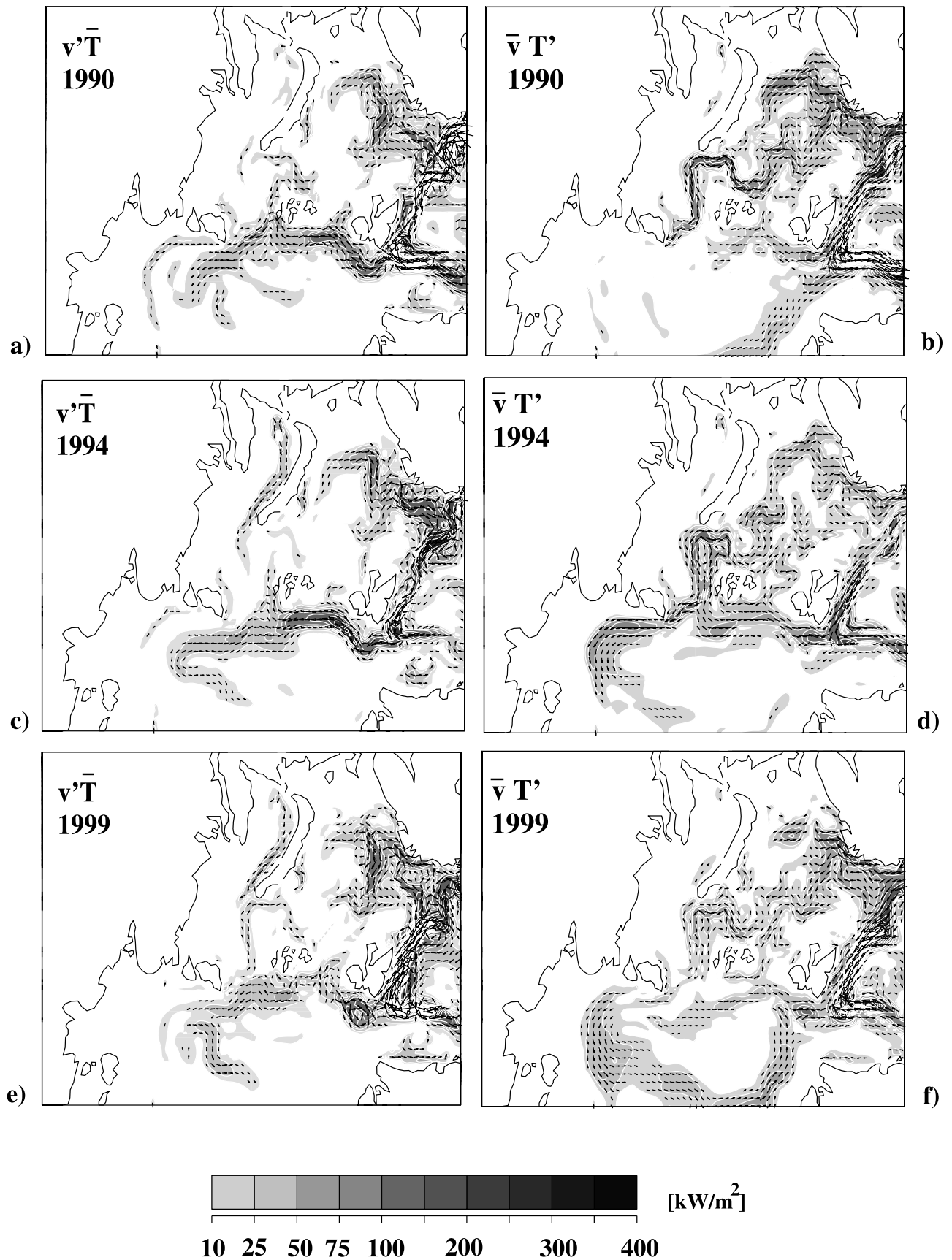


Figure 6. Contributions of (left-hand column) anomalous velocity and (right-hand column) temperature to the depth integrated (100–300 m) horizontal heat flux in the 1990s.

Barents Sea in 1990 (Figure 6b). Anomalously warm Barents Sea Branch Water reached St. Anna Trough. It proceeded into the basin in the following years. At the confluence of the two Atlantic Water branches north of St. Anna Trough in 1990 FSBW and BSBW contributed both to an increased eastward heat transport of the boundary current into the eastern Eurasian Basin with anomalous speed and anomalous temperature, respectively. It was not until 1993, however, that the temperature anomaly advected from Fram Strait reached St. Anna Trough to add to the still anomalously warm BSBW flow. In 1994, then, the entire boundary current from Fram Strait to the Laptev Sea slope and back poleward along the Lomonosov Ridge, exhibited anomalously swift and warm flow (Figures 6c and 6d). In the western Barents Sea, temperature and velocity by this time had switched back to cold and weak conditions, respectively. At the end of the 1990s an anomalously swift and warm flow of the WSC and of water crossing the Barents Sea prevailed again.

[23] At the Barents Sea Opening (BSO), where the Barents Sea branch started its shelf passage, several cold and warm phases were discernible in model data and observations (Figures 3b and 4b). Two short warm periods took place in 1979/1980 and 1984/1985, which we term BSO-W1, since in the data the first of these is very weak. A long warm period lasted from 1989 to 1993 (BSO-W2). The water of the Barents Sea branch crossed the shelf eastward along meandering paths guided by the local topography. After passing the gap between Franz-Josef-Land and Novaja Semlja, the denser part of the water flowed northward along the eastern flank of St. Anna Trough forming the source for the BSBW. The temperatures of the Barents Sea branch just before it entered the trough were reduced by several degrees centigrade as compared to the BSO location (compare Figures 4b and 4c). Responsible for this cooling was the intense heat loss to the atmosphere taking place in the eastern Barents Sea [Gerdes, 2000; Karcher and Oberhuber, 2002]. This is also evident in the 21 years mean total surface heat flux shown in Figure 11a below. The variability of temperature in the Barents Sea branch north of Novaja Semlja, however, was still in the range of 0.5° – 1° C. Warm periods around 1985 and after 1989 are obvious. The temperature maxima around 1985 and in the early 1990s, as well as the relative minima in the early and late 1980s, apparently were caused by the upstream temperatures at the BSO. The reduction of BSO inflow temperatures by 0.8° C from 1992 to 1997 (BSO-C2), however, had no counterpart of comparable amplitude at the downstream location (Figure 4c). The resulting temperature time series for the Barents Sea branch source water passing the Franz-Josef-Land-Novaja Semlja gap exhibited rather high Atlantic Water temperatures for the entire 1990s with peaks in 1993 and 1997. In the trough the BSBW started mixing with FSBW which entered the trough on its western flank. The end product mixed with the FSBW core at the shelf break after leaving the trough. Further east at the slope near Svernavja Semlja the temperature at 350 m depth (Figure 5b) reveals a weak warming peak in 1985/1986 due to the influence of less cold shelf water and a following temperature minimum in 1987/1988 due to colder shelf water (compare Figure 4c). The strong temperature rise in the late 1980s to early 1990s near Svernavja Semlja (Figure 5b) by about 1.2° C reflects the combined influence of the slow FSBW warming trend as found in the FSBW core upstream near Franz-Josef-

Land (Figure 5a) and the abrupt warming of the BSBW after 1988 (Figure 4c).

[24] By 1993 the temperature anomaly in the boundary current had not only started to recirculate in the Amundsen Basin along the Lomonosov Ridge but had begun to intrude the Makarov Basin beyond the ridge (Figure 2e). The Atlantic Water core temperature at the continental slope of the Makarov Basin rose by about 1° C in the mid-1990s as compared to the previous decade (Figure 2f). The model suggests spreading of the warm anomaly in the Atlantic Water layer across the Lomonosov Ridge not only near the continental slope but also further north. In the second half of the 1990s the Siberia Abyssal Plain between the Lomonosov and Alpha Ridges warmed due to a spill over of Atlantic Water from the Eurasian Basin up to 1.6° C (Figures 2g and 2h). During this period the anomalously warm water branch at the continental slope advanced further eastward to the slope of the Chukchi Plateau. In 1999 the model shows core temperatures of up to 0.8° C there, very similar to observations (Figure 2h). By then the first signs of the warm anomaly traveling with the branch along the Lomonosov Ridge reached the western Eurasian Basin north of Fram Strait. Thus for the last decade of the simulation we find a travel time of the anomaly from Franz-Josef-Land to northern Fram Strait of about 10 years. While the anomalously warm water had been advancing along Lomonosov Ridge and along the continental slope of the Makarov Basin, the boundary current temperatures at the Barents Sea slope have been cooling down again to values of about 2° C in 1999 (Figures 2g and 2h) due to cooler upstream temperatures after 1995 in the West Spitsbergen Current (Figure 4a).

[25] The modeled Atlantic Water core temperatures in the boundary current of the Arctic Ocean, their structure and development are generally in good agreement with the available observations. The interior Eurasian Basin, however, is colder than the observations. This may be a consequence of rather cold temperatures in the interior Eurasian Basin at the beginning of the experiment in 1979. In fact during the 20 year spin-up run forced with a 1979–1994 climatology (see section 2) the Barents Sea Branch Water had been considerably colder than in most of the years 1979–1999 in the following hindcast experiment.

[26] From the model results and the available measurements we conclude that the development of the Atlantic Water core temperature in the boundary current of the Eurasian Basin and parts of the Makarov and Canadian Basins between 1979 and 1999 took place in the form of events. As a consequence, the large-scale pattern of the Atlantic Water core temperature at the end of the 1990s is characterized by a large patch of anomalously warm water in the Atlantic Layer stretching along the Lomonosov Ridge and the slopes of the Canadian and Makarov Basins. The temperatures of the Atlantic Water core in the boundary current along the Barents and Kara Sea slope, on the other hand, has returned to markedly cooler conditions than in the first half of the 1990s.

[27] From the comparison of the model temperatures with observations we are able to conclude both Atlantic Water branches, FSBW and BSBW, had an influence on the evolution of the boundary current temperatures in the Arctic Ocean. As became evident by the first small warm anomaly of the 1980s which got stuck north of Franz-Josef-Land, as compared to the swift spreading of the early 1990s warm

anomaly, the boundary currents which carry the temperature signals do not act in a steady or continuous fashion.

4. Horizontal Fluxes and Heat Balance

[28] In the following section we will trace back the anomalously warm inflow of the mid-1980s and the 1990s to the lateral heat and volume fluxes through the major straits connecting the Arctic Ocean, the Nordic Seas and the northern North Atlantic. The fluxes are calculated as vertically integrated winter-centered means (July–June). We are well aware that it is not possible to calculate heat fluxes from single sections. Instead we calculated temperature fluxes relative to a reference temperature which we defined as -0.1°C . In the following we will use the phrase “heat flux” for this temperature flux relative to the reference value. Named years stand for the winter-centered mean which ends in the respective year, for example, 1995 for the winter-centered year July 1994 through June 1995. The locations of the sections are depicted in Figure 1. We will also identify the large-scale patterns of the upper 500 m horizontal heat fluxes which are associated with the heat fluxes through Fram Strait and the BSO. Finally we discuss the windstress patterns which are associated with the time series of volume fluxes through the straits.

4.1. Horizontal Heat and Volume Fluxes

[29] The volume flux into the Arctic Ocean via Fram Strait (Figure 7a, medium shaded columns) fluctuates inter-annually between 2 and 3 Sv. The 1990s are characterized by an inflow which is about 0.5–1 Sv higher than in most of the 1980s. The net heat inflow (Figure 7a, black columns) also shows a higher level in the 1990s. The larger increase of the heat flux as compared to the volume flux in the period 1990 to 1995 reflects higher temperatures of the inflowing water. Maximum heat fluxes from 1993 to 1995 reach more than 25 TW, which is about 10–15 TW above the level of the 1980s. Volume and heat inflow are reduced again in the second half of the 1990s. The volume and heat transport entering the Barents Sea via the BSO (Figure 7b, medium shaded and black columns, respectively) are at maximum in the years 1980, 1983 and 1984, and from 1989 to 1993 when heat transports of 50–60 TW are reached. In contrast, the heat input during the weak periods amounts to 40–45 TW. A reduced heat transport is found in the mid-1990s. An increase of heat transport occurs again after 1997. While for the volume transports it is evident that the amount of water entering the Barents Sea via the BSO has to leave it toward the Arctic Ocean proper via the Arctic Barents Sea Connection (ABC), the heat transport through the BSO and the ABC are decoupled (Figure 7c, medium shaded and black columns, respectively). For the ABC section the volume transport is shown positive into the Arctic Ocean proper, the heat transport has a negative sign due to potential temperatures below the reference value. Maximum heat transport into the Arctic Ocean is taking place in 1985/1986 and from 1990 to 1996, with 5–8 TW above the level of the first half of the 1980s.

[30] The depth integrated yearly mean northward transport of Atlantic water between Iceland and the Faroe Islands fluctuates between 3 and 4 Sv. This is consistent with observations of the Atlantic Water fraction rounding

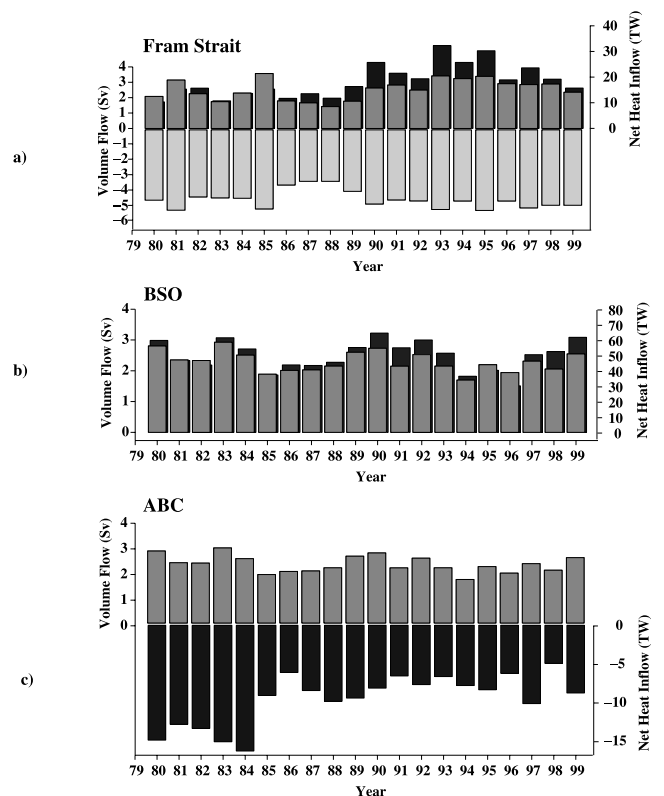


Figure 7. Winter-centered (July–June) yearly means of net volume (medium shading) and heat inflow (black) for the major entrances of Atlantic Water to the Arctic Ocean: (a) Fram Strait, (b) the Barents Sea Opening (BSO) and (c) the Arctic Barents Sea Connection (ABC). For Fram Strait the net inflow (medium shading) and outflow (light shading) of volume are shown separately. The locations of the sections are shown in blue in Figure 1.

the northern tip of the Faroes [Hansen and Østerhus, 2000]. In the model a yearly mean southward flow of about 1 Sv reduces the net northward flow to 3–4 Sv (Figure 8a). The yearly mean net northward heat transport across this gap behaves almost parallel to the volume flux and amounts to about 70 TW with maxima of about 80 TW in 1989–1990 and 1998–1999. The situation is different for the Faroe-Scotland gap, where the yearly northward volume transport exhibits a higher interannual variability of about 3–4.5 Sv and a rather constant 0.6 Sv southward transport (Figure 8b). The depth integrated net volume transport to the north increases from a low of 2–3 Sv in the second half of the 1980s to values of 3–4 Sv from 1989 to 1995, mainly due to intensified northward transport in the winter months (not shown). The net northward heat transport mirrors the volume transport, showing an increase from a low in the late 1980s of about 100 TW to a maximum of 120–140 TW in the first half and at the end of the 1990s. It is noteworthy that both sections show a strong decrease of net northward heat and volume transports in the year 1995/1996, with a swift recovery of the heat transports afterwards to values found in the first half of the decade.

[31] Summing up, we find an increased northward flow of volume and heat across the Iceland–Scotland ridge from 1989 to 1995. Each of the two gates to the Arctic Ocean

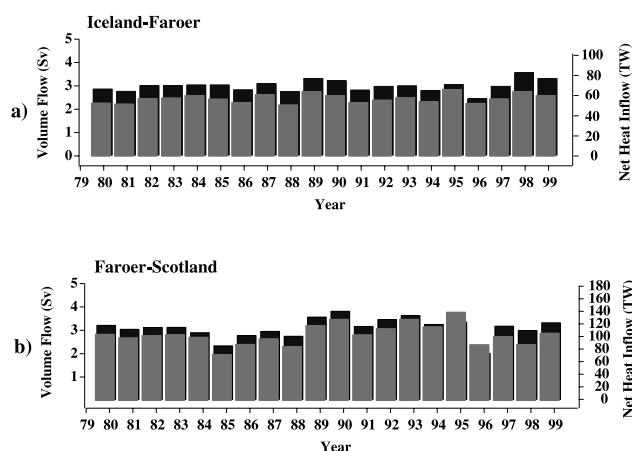


Figure 8. Winter-centered (July–June) yearly means of net volume and heat inflow for the main entrances of Atlantic Water to the Nordic Seas: (a) the Iceland-Farøer section and (b) the Farøer-Scotland section. The locations of the sections are shown in blue in Figure 1.

filter out a different period of maximum inflow from this period, the Barents Sea Opening leading Fram Strait by 1 to 2 years.

4.1.1. Associated Horizontal Heat Transport Patterns

[32] For a better understanding of the large-scale patterns of heat transport in the ocean we calculate the pattern of horizontal heat flux anomalies integrated over the upper 500 m of the water column which are associated with the net heat transport through the Fram Strait and BSO sections (Figure 7). Large (northward) heat transport through Fram Strait (Figure 9a) is associated with an intensified horizontal heat flux of the West Spitsbergen Current. Large (northward) heat transport through the strait is associated also with a slight northward shift of the recirculation of Atlantic Water in its southern area. Recirculation and West Spitsbergen Current are fed by almost equal contributions of outer and inner branch of the Norwegian Atlantic Current and the Norwegian Coastal Current. These in turn are fed by an increase of horizontal heat flux across the Farøer-Scotland Ridge which is concentrated on the Scottish side. The latter also holds for the heat transport patterns associated with increased heat transport through the BSO section (Figure 9b). In addition it is associated with an increase of horizontal heat flux across the Iceland-Farøer section which feeds the outer branch of the Norwegian Atlantic Current. An intensified northward heat flux is carried with the outer part of the West Spitsbergen Current which feeds an intensified and southward shifted recirculation of Atlantic Water in southern Fram Strait.

4.1.2. Associated Windstress Patterns

[33] In the following, the fields of winter-centered yearly means of windstress have been regressed on the winter-centered yearly mean transports of volume through the straits which have been discussed above. A large northward volume transport through Fram Strait is associated with a cyclonic windstress anomaly over the central Arctic Ocean and the northern Nordic Seas (Figure 10a). Typical correlation coefficients for the large scale stress pattern shown are 0.4–0.6 (for the correlations given in this section, a

coefficient of $|\rho| > 0.55$ is statistically significant at the 95% level). Interestingly, there is no indication for a strong influence of the local windfield on the variability of the throughflow on these interannual timescales. Instead, the local windstress pattern over Fram Strait is directed south-eastward and tends to promote an intensified southward transport with the East Greenland Current. The intensified East Greenland Current in turn requires a stronger northward transport with the West Spitsbergen Current. For an intensified eastward BSO volume transport the associated wind stress pattern (Figure 10b) exhibits strong cyclonicity over the central Nordic Seas. This pattern will tend to increase the cyclonic flow in the entire Nordic Seas. Due to northwestward windstress in the vicinity of the BSO, the Ekman transport also supports intense throughflow of the

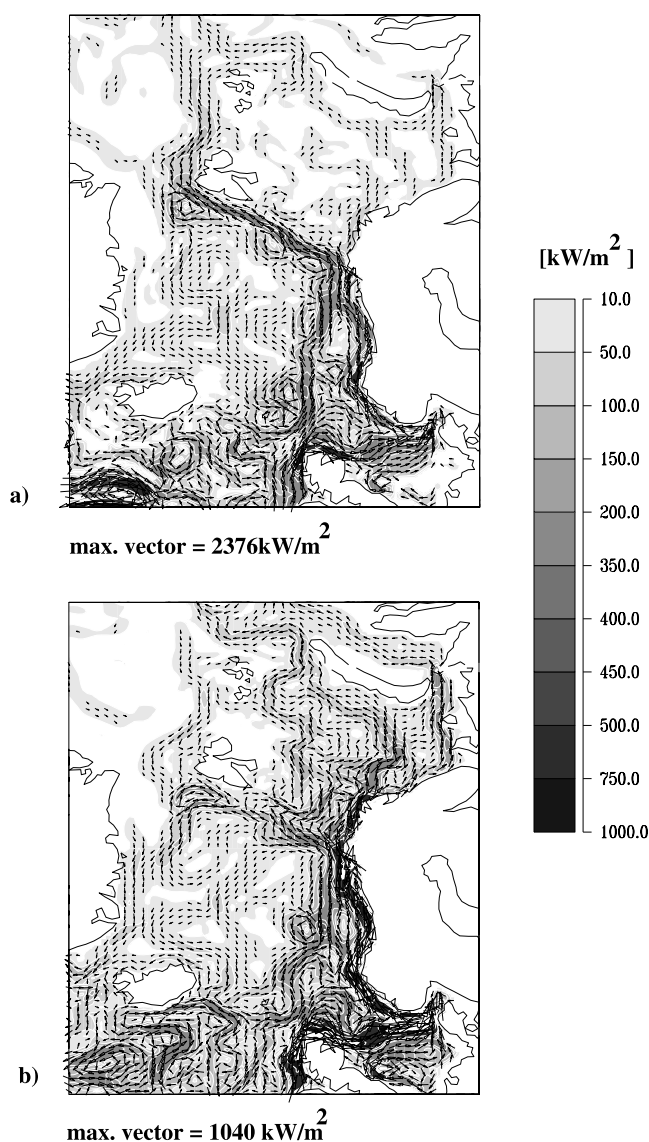
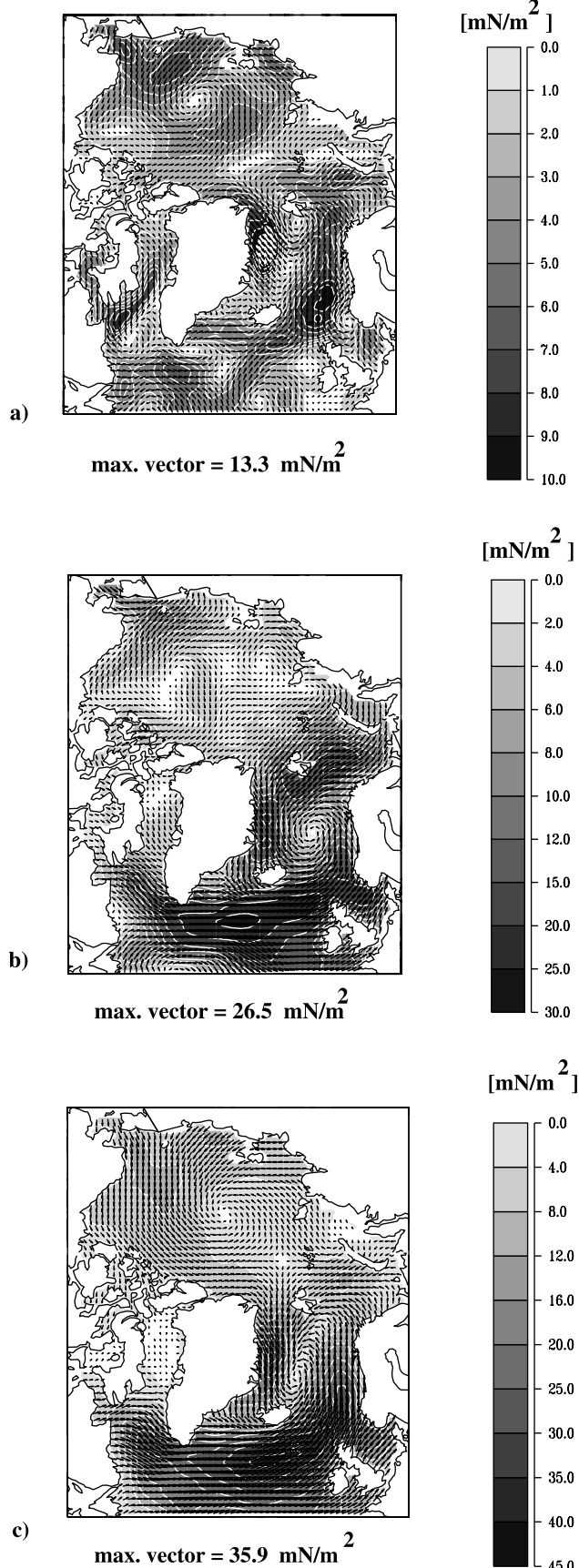


Figure 9. The horizontal heat flux (relative to -0.1°C) pattern integrated over the upper 500 m watercolumn which is associated with the time series of net heat transport from the Nordic seas (a) into the Arctic Ocean via Fram Strait (Figure 7a) and (b) into the Barents Sea across the BSO section (Figure 7b).



Barents Sea. We find intensified westerlies in the atmosphere over the northern North Atlantic, as we would expect for an intensified NAO. The intensification of the large-scale Atlantic Water recirculation of the Nordic Seas found in the associated horizontal heat flux pattern (Figure 9b) is consistent with the associated windstress pattern (Figure 10b) which exhibits an increased cyclonicity over the central Nordic Seas. The typical correlation for the large scale pattern is 0.5–0.6. The windstress patterns which are associated with the northward volume transports across the Iceland-Farøer (not shown) and Farøer-Scotland (Figure 10c) sections are very similar with each other. Both exhibit increased westerlies in the northern North Atlantic, a strong cyclonicity over the Nordic seas with the center north of Iceland and cyclonic tendency over the Arctic Ocean. Here the typical correlation is 0.5–0.7. This pattern is in accordance with the notion of intensified northward volume transport of Atlantic Water across the Iceland-Scotland ridge system in the early 1990s, as anticipated, for example, by *Dickson et al.* [2000].

4.2. Heat Balances

[34] In the following section we will calculate heat balances for relevant areas of the Nordic Sea and the Eurasian Shelf to quantify the contributions of anomalous surface heat fluxes and lateral heat fluxes to the development of the 1990s warm anomaly. We analyzed heat balances for three boxes covering relevant areas along the Atlantic Water pathway from the Iceland-Scotland Ridge to the Arctic Ocean (Figure 11a). Box A covers the Norwegian Atlantic Current and Norwegian Coastal Current in the eastern Nordic Seas from the Iceland-Scotland Ridge to the West Spitsbergen Current. Box B covers the northern West Spitsbergen Current and the recirculation area of the return Atlantic Water south of Fram Strait. Box C covers the Barents and Kara Seas. The underlying coloring shows the mean total heat flux at the surface of the ocean (positive = upward heat flux) from 1979 to 1999. Large heat loss along the path of the Atlantic Water in the Nordic Seas, with maxima in the northern parts, the West Spitsbergen Current and its recirculation and in the Barents Sea is apparent.

[35] The net heat transport anomaly entering box A with the North Atlantic Current (NAC) (black) amounts to about 40 TW between 1989 and 1995 as compared to the previous decade. Furthermore, from 1988 to 1992, box A experiences a reduced heat loss to the atmosphere of about 10 TW, as compared to the previous decade (Figure 11b). Of this heat an anomalous plus of 15–20 TW enter the Barents Sea box C via the BSO section (yellow) and a plus of 20–25 TW the WSC/recirculation box B (blue) in the early 1990s.

[36] A comparison of sea surface temperature and total surface heat fluxes (not shown) reveals that for the early 1990s in box A, especially in the southeastern Nordic Seas and the North Sea, high sea surface temperature and reduced heat loss to the atmosphere are in phase, forced by an

Figure 10. (opposite) Surface windstress pattern associated with the time series of volume transport (a) northward across the Fram Strait section (Figure 7a), (b) eastward across the BSO section (Figure 7b), and (c) northward across the Iceland-Farøer section (Figure 8a).

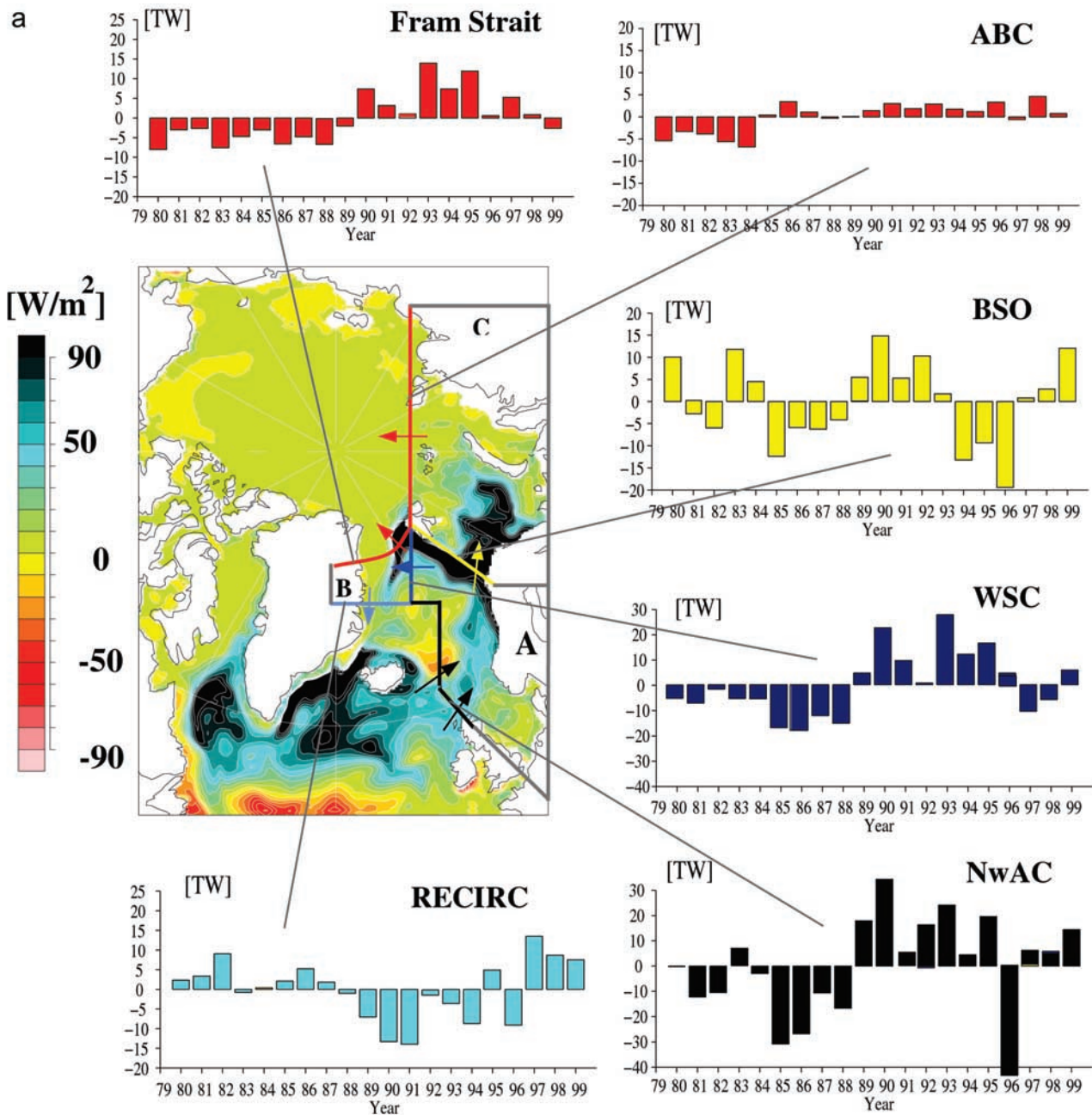


Figure 11. Heat balances for three boxes (A, B, C) covering the pathway of Atlantic Water in the Nordic Seas and the Barents/Kara Seas. (a) The underlying map in the central frame shows the mean total ocean surface heat flux from 1979 to 1999 (positive = upward heat flux). Heat flux in excess of 90 TW/m^2 is shown in black. The colored arrows sketch the mean flow direction of the Atlantic Water. The lateral heat transport anomalies across the boundaries of the boxes are shown as columns in the diagrams around the central frame and are correspondingly colored. The transport anomalies are shown positive into the direction of the arrows. (b) The total surface heat flux anomalies for each of the three boxes shown as columns. All data are winter-centered yearly means (July–June).

anomalously warm surface air temperature. This result is consistent with conclusions drawn from observed data [Furevik, 2001]. In contrast to this, the other areas namely the Barents Sea (box C) and the West Spitsbergen Current/recirculation region (box B) show sea surface temperature and total surface heat flux out of phase, characterizing a damping of the advected sea surface temperature anomalies by intensified heat loss to the atmosphere.

[37] During the early 1990s in box B strong heat loss to the atmosphere (Figure 11b) and a strong recirculation in southern Fram Strait (RECIRC, light blue, Figure 11a) reduce the heat surplus available for finally entering the Arctic Ocean proper via Fram Strait (red) (Figure 11a). Still, the supply of additional heat to the Arctic via Fram Strait is increased by 10–15 TW between 1989 and 1995. For the Barents and Kara Seas (box C) the heat surplus which had

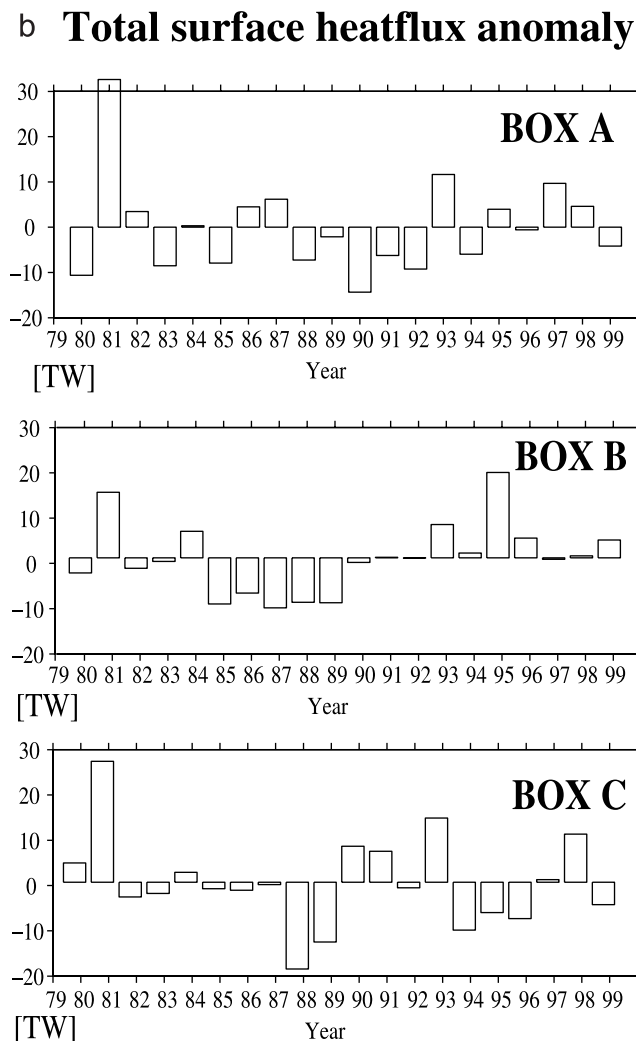


Figure 11. (continued)

entered via the BSO section (yellow) between 1989 and 1993 has been reduced to about 10 TW at the ABC outflow section (red). Thus, even though on the shelf the atmospheric damping has reduced the available heat surplus to about one third of the original inflow, significant interannual variations remain to enter the Arctic Ocean proper. This was evident also from the temperature time series which had shown 0.5° – 1° C interannual variability in the outflowing deep shelf water between Franz-Josef Land and Novaya Semlya (Figure 3c). The BSBW exiting the shelf via St. Anna Trough showed up to 1° C higher temperatures in the early to middle 1990s than in the first half of the 1980s. It is a total surplus of about 30 TW of heat which entered the Arctic Ocean proper with the Fram Strait branch and the Barents Sea branch of Atlantic Water in the early 1990s and formed the Arctic Ocean warm event of the 1990s.

5. Conclusions

[38] Since 1991, measurements reveal a warming of the Atlantic Layer of the Arctic Ocean [Quadfasel *et al.*, 1991]. The intensity, extent and sources of this warming have been the subject of discussion in the oceanographic literature ever

since. Due to the patchy nature of observational data in space and time, a consistent picture of the development of the Atlantic Water temperature over the last 2 decades and its relation to conditions in the Nordic Seas has not been possible so far. Here we used a coupled ice-ocean model driven with atmospheric data from the period 1979 to 1999 to discuss the characteristics of this warming and try to develop a consistent picture of the variability of the Atlantic Water heat and volume fluxes in the Arctic Ocean and the Nordic Seas. Furthermore, we discuss the possible mechanism responsible for the nature of the warming and its connection with other phenomena observed in the Arctic Ocean during the same period.

[39] The model hindcast reproduces the observed development and subsequent northward propagation of temperature anomalies in the water of Atlantic origin in the Northwest European Shelf area and along the Norwegian coast. The model clearly depicts the strong warming of the Atlantic Water boundary current in the Arctic Ocean beginning in the early 1990s.

[40] The model results reveal that instead of being a steady process, the evolution of the Atlantic Layer warming occurs in the form of events, triggered by changes in the inflowing water through Fram Strait and the Barents Sea, and modified by changes in the local current speeds. Two such events are captured during the 2 decades of the hindcast simulation. A first weak warming event occurred in the early 1980s. It was restricted to the western Eurasian Basin due to a weaker cyclonic circulation of the boundary current. A second large warming event starting in the late 1980s/early 1990s lead to a widespread temperature increase extending far into the eastern Eurasian Basin and across the Lomonosov Ridge into the western Arctic basins. The source of the much larger second warm event was an increase of volume inflow across the Faroer-Scotland Ridge into the Nordic Seas due to a changed wind stress pattern. It delivered an additional 30–40 TW in the first half of the 1990s in comparison to the earlier period. It was backed up by another 10 TW which were available due to anomalously warm surface air temperatures in the eastern Nordic Seas and the North Sea resulting in reduced surface heat loss.

[41] This results in an additional inflow of heat of about 30 TW into the Arctic Ocean proper in comparison to the 1980s. It is advected by an intensified boundary current system from the Nordic Seas into the Arctic basins. The major part (three quarters) of this surplus heat input entered through Fram Strait. A smaller contribution (one quarter) was a reduced heat loss of the Arctic Ocean proper because of an inflow of less cold water from the Barents Sea. From the comparison of the model results with observations we are able to conclude that the temperature of the inflowing Atlantic Water at Fram Strait has a major influence on the temperature evolution of the boundary currents of the interior basins.

[42] As became evident following a first slowly propagating warm anomaly in the early 1980s in comparison to the swift spreading of the 1990s warm event, the boundary currents do not act in a steady or continuous fashion. The 1990s anomalous cyclonicity in the Arctic Ocean wind stress pattern not only had a strong impact on the intensity of the boundary currents in the Arctic Ocean interior, but

also was associated with an increased Atlantic Water inflow volume which entered through Fram Strait. Even though the general increase of heat and volume transports during the high NAO years in the early 1990s is evident in both straits (the Fram Strait and the BSO), they differ in the response to interannual variability of regional wind stress patterns over the Nordic Seas and the central Arctic. The time series of volume transport through the BSO and the two Iceland-Faroe-Scotland sections and their associated windstress patterns are similar and exhibit a stronger correlation with the NAO index than the same parameters for the Fram Strait section.

[43] In the second half of the 1990s reduced temperatures of the inflowing water and a reduced volume inflow are shown by the model hindcast. Thus at present the Arctic warm event of the 1990s is advected through the Arctic basins as an isolated positive temperature anomaly. In 1999, increasing temperatures in the Atlantic Water of the Nordic Seas approaching the Arctic Ocean are apparent again from measurements and the model hindcast. We therefore expect the occurrence of a new warm event in the western Eurasian Basin and the western Barents Sea in the next years.

[44] **Acknowledgments.** The authors would like to express their gratitude toward the agencies which funded part of this work: the European Union under EC MAST III programme through grant MAS3-CT96-0070 (VEINS), and the German Ministry for Education and Research (BMBF) through grant 01 LA 9823/7. This material is based upon work partially supported by the National Science Foundation under agreement OPP-0002239 with International Arctic Research Center, University of Alaska Fairbanks (Arctic Ocean Model Intercomparison Project). Any opinions, findings, and conclusions or recommendations expressed in this material are those of the author(s) and do not necessarily reflect the views of the National Science Foundation. Thanks also to Matthias Klawa from the University of Cologne, for help with the windstress data, and to two anonymous reviewers for fruitful comments on the manuscript.

References

- Anderson, L. G., and E. P. Jones, Tracing upper waters of the Nansen Basin in the Arctic Ocean, *Deep Sea Res.*, **39**, 425–433, 1992.
- Anderson, L. G., E. P. Jones, K. P. Koltermann, P. Schlosser, J. Swift, and D. W. R. Wallace, The first oceanographic section across the Nansen Basin in the Arctic Ocean, *Deep Sea Res., Part A*, **36**, 475–482, 1989.
- Anderson, L. G., G. Bjoerk, O. Hoby, E. P. Jones, G. Kattner, K. P. Koltermann, B. Liljebld, R. Lindegren, B. Rudels, and J. Swift, Water masses and circulation in the Eurasian Basin: Results from the Oden 91 expedition, *J. Geophys. Res.*, **99**, 3273–3288, 1994.
- Carmack, E. C., R. W. MacDonald, R. G. Perkin, F. A. McLaughlin, and R. J. Pearson, Evidence for warming of Atlantic Water in the southern Canadian Basin of the Arctic Ocean: Results from the Larson-93 expedition, *Geophys. Res. Lett.*, **22**, 1061–1064, 1995.
- Dickson, R. R., All change in the Arctic, *Nature*, **397**, 389–390, 1999.
- Dickson, R. R., T. J. Osborn, J. W. Hurrell, J. Meincke, J. Blindheim, B. Adlandsvik, T. Vinje, G. Alekseev, and W. Maslowski, The Arctic Ocean response to the North Atlantic Oscillation, *J. Clim.*, **15**, 2671–2696, 2000.
- Furevik, T., Annual and interannual variability of Atlantic Water temperatures in the Norwegian and Barents Seas: 1980–1996, *Deep Sea Res., Part I*, **48**, 383–404, 2001.
- Gerdes, R., Modelling the variability of exchanges between the Arctic Ocean and the Nordic Seas, in *The Freshwater Budget of the Arctic Ocean*, edited by L. E. Lewis, pp. 553–547, Kluwer Acad., Norwell, Mass., 2000.
- Gerdes, R., C. Köberle, and J. Willebrand, The influence of numerical advection schemes on the results of ocean general circulation models, *Clim. Dyn.*, **5**, 211–226, 1991.
- Gibson, J. K., P. Kallberg, S. Uppala, A. Nomura, E. Serrano, and A. Hernandez, ERA description: ECMWF reanalysis project report 1: Project organisation, Eur. Cent. for Medium Range Weather Forecast, Reading, England, 1997.
- Gorshkov, S. G., Atlas of Oceans: Arctic Ocean, Mil. Defence Publ. House, Moscow, 1980.
- Grotefendt, K., K. Logemann, D. Quadfasel, and S. Ronski, Is the Arctic Ocean warming?, *J. Geophys. Res.*, **103**, 27,679–27,687, 1998.
- Häkkinen, S., and C. A. Geiger, Simulated low-frequency modes of circulation in the Arctic Ocean, *J. Geophys. Res.*, **105**, 6549–6564, 2000.
- Hansen, B., and S. Østerhus, North Atlantic-Nordic Seas exchanges, *Prog. Oceanogr.*, **45**, 109–208, 2000.
- Harder, M., P. Lemke, and M. Hilmer, Simulation of sea ice transport through Fram Strait: Natural variability and sensitivity to forcing, *J. Geophys. Res.*, **103**, 5595–5606, 1998.
- Hibler, W. D., A dynamic thermodynamic sea ice model, *J. Phys. Oceanogr.*, **9**, 815–846, 1979.
- Hibler, W. D., III, and K. Bryan, A diagnostic ice-ocean model, *J. Phys. Oceanogr.*, **17**, 987–1015, 1987.
- Holloway, G., and T. Sou, Has Arctic sea ice rapidly thinned?, *J. Clim.*, **15**, 1692–1701, 2001.
- Hurrell, J. W., Decadal trends in the North Atlantic Oscillation: Regional temperatures and precipitation, *Science*, **269**, 676–679, 1995.
- Johnson, M. A., and I. V. Polyakov, The Laptev Sea as a source for recent Arctic Ocean salinity changes, *Geophys. Res. Lett.*, **28**, 2017–2020, 2001.
- Karcher, M. J., and J. M. Oberhuber, Pathways and modification of the upper and intermediate water of the Arctic Oceans, *J. Geophys. Res.*, **107**, 3049, 10.1029/2000JC000530, 2002.
- Köberle, C., and R. Gerdes, Causes of Arctic sea ice volume variability, *J. Clim.*, in press, 2003.
- Koltermann, K. P., and H. Lühje, Hydrographic atlas of the Greenland and northern Norwegian seas, Dtsch. Hydrogr. Inst., Hamburg, Germany, 1989.
- Levitus, S., R. Burgett, and T. Boyer, World Ocean Atlas 1994, vol. 3, Salinity, *NOAA Atlas NESDIS 3*, U.S. Dep. of Comm., Washington D. C., 1994a.
- Levitus, S., R. Burgett, and T. Boyer, World Ocean Atlas 1994, vol. 4, Temperature, *NOAA Atlas NESDIS 4*, U.S. Dep. of Comm., Washington D. C., 1994b.
- Maslowski, W., D. C. Marble, W. Walczowski, and A. J. Semtner, On large scale shifts in the Arctic Ocean and Sea Ice conditions during 1979–1998, *Ann. Glaciol.*, **33**, 545–550, 2001.
- McLaughlin, F. A., E. C. Carmack, R. W. Macdonald, and J. K. B. Bishop, Physical and geochemical properties across the Atlantic/Pacific water mass front in the southern Canadian basin, *J. Geophys. Res.*, **101**, 1183–1197, 1996.
- Morison, J., M. Steele, and R. Andersen, Hydrography of the upper Arctic Ocean measured from the nuclear submarine Pargo, U.S.S., *Deep Sea Res.*, **45**, 15–38, 1998.
- Muench, R. D., M. G. McPhee, C. A. Paulson, and J. H. Morison, Winter oceanographic conditions in the Fram Strait-Yermak Plateau region, *J. Geophys. Res.*, **97**, 3469–3483, 1992.
- NSIDC Environmental Working Group, Joint U.S. Russian Atlas of the Arctic Ocean: Oceanography Atlas for the Winter Period [CD-ROM], Univ. of Colo., Boulder, 1997.
- Pacanowski, R. C., MOM 2 Documentation, user's guide and reference manual, *GFDL Ocean Group Tech. Rep. 3*, Geophys. Fluid Dyn. Lab., Princeton Univ., Princeton, N. J., 1995.
- Perkin, R. G., and E. L. Lewis, Mixing in the West Spitsbergen Current, *J. Phys. Oceanogr.*, **14**, 1315–1325, 1984.
- Quadfasel, D., A. Sy, D. Wells, and A. Tunik, Warming in the Arctic, *Nature*, **350**, 385, 1991.
- Rigor, I. G., R. L. Colony, and M. Seelye, Variations in surface air temperature observations in the Arctic, 1979–97, *J. Clim.*, **13**, 896–914, 1997.
- Röske, F., An atlas of surface fluxes based on the ECMWF Re-Analysis-A climatological dataset to force global ocean general circulation model, *MPI-Rep. 323*, Max-Planck-Inst. für Meteorol., Hamburg, Germany, 2001.
- Rudels, B., The T-S relations in the northern seas: Implications for the deep circulation, *Polar Res.*, **4**, 133–159, 1986.
- Rudels, B., R. D. Muench, J. Gunn, U. Schauer, and H. J. Friedrich, Evolution of the Arctic Ocean boundary current north of the Siberian Shelves, *J. Mar. Syst.*, **25**, 77–99, 2000.
- Schauer, U., R. D. Muench, B. Rudels, and L. Timokhov, The impact of eastern Arctic shelf waters on the Nansen Basin, *J. Geophys. Res.*, **102**, 3371–3382, 1997.
- Schauer, U., B. Rudels, P. Jones, L. G. Anderson, R. D. Muench, G. Bjork, J. H. Swift, V. Ivanov, and A.-M. Larsson, Confluence and redistribution of Atlantic Water in the Nansen, Amundsen and Makarov basins, *Ann. Geophys.*, **20**, 257–273, 2002.
- Semtner, B., A model for the thermodynamic growth of sea ice in numerical investigations of climate, *J. Phys. Oceanogr.*, **6**, 379–389, 1976.
- Sokolov, V., S. Pivovarov, and W. Schneider, Oceanography, chap. 7, in *ARCTIC '98: The Expedition ARK-XIV/1a of RV 'Polarstern' in 1998*, *Rep. on Polar Res. 308*, Alfred Wegener Inst. für Polar- und Meeresforschung, Bremerhaven, Germany, 1999.

- Steele, M., and T. Boyd, Retreat of the cold halocline layer in the Arctic Ocean, *J. Geophys. Res.*, *103*, 10,419–10,435, 1998.
- Steele, M., J. H. Morison, and T. B. Curtin, Halocline water formation in the Barents Sea, *J. Geophys. Res.*, *100*, 881–894, 1995.
- Steele, M., W. Ermold, G. Holloway, S. Häkkinen, D. Holland, M. Karcher, F. Kauker, W. Maslowski, N. Steiner, and J. Zhang, Adrift in the Beaufort Gyre: A Model intercomparison, *Geophys. Res. Lett.*, *28*, 2838–2935, 2001.
- Stevens, D. P., The open boundary condition in the United Kingdom Fine-Resolution Antarctic Model, *J. Phys. Oceanogr.*, *21*, 1494–1499, 1991.
- Swift, J. H., E. P. Jones, K. Aagaard, E. C. Carmack, M. Hingston, R. W. Macdonald, F. A. McLaughlin, and R. G. Perkin, Waters of the Makarov and Canada basins, *Deep Sea Res., Part II*, *44*, 3371–3382, 1996.
- Walsh, J. E., W. L. Chapman, and T. L. Shy, Recent decrease of sea level pressure in the central Arctic, *J. Clim.*, *9*, 480–486, 1996.
- Zalesak, S. T., Fully multidimensional flux-corrected transport algorithms for fluids, *J. Comput. Phys.*, *31*, 335–362, 1979.
- Zhang, J., D. A. Rothrock, and M. Steele, Warming of the Arctic Ocean by a strengthened Atlantic inflow: Model results, *Geophys. Res. Lett.*, *25*, 1745–1748, 1998.
-
- R. Gerdes, M. J. Karcher, F. Kauker, and C. Köberle, Alfred-Wegener Institute for Polar and Marine Research, Bussestrasse 24, P.O. Box 120161, 27515 Bremerhaven, Germany. (rgerdes@awi-bremerhaven.de; mkarcher@awi-bremerhaven.de; fkauker@awi-bremerhaven.de; ckoeberl@awi-bremerhaven.de)